

Estimation of the probability distributions for cable coupling using unscented transforms

David W. P. Thomas · Leonardo R. A. X. de Menezes ·
Christos Christopoulos · Frank Leferink ·
Hans J. G. Bergsma

Received: 26 November 2009 / Accepted: 13 April 2011
© Institut Télécom and Springer-Verlag 2011

Abstract This work presents the use of unscented transforms (UT) for the description of statistical uncertainty in electromagnetic coupling between cables. UT greatly reduce the computational burden for the statistical analysis of nonlinear problems compared with more traditional approaches such as the Monte Carlo technique. Coupling between cables has a nonlinear parameter dependence and has a high variability due to the variability in the cable braid manufacture and the highly variable nature of cable layout. Therefore, cable coupling can only be defined within statistical limits. First, it is shown that by analyzing the resonances the important features of maximum coupling and the point of maximum coupling can be characterized. It is then demonstrated how UT can be used to efficiently identify the parameters which contribute significantly to the

uncertainty in cable coupling and then to provide a measure of the probability distribution for the multivariate problem.

Keywords Unscented transforms · Statistical analysis · Cable coupling · EMC

1 Introduction

Nondeterministic problems are challenging in electromagnetic compatibility (EMC) analysis. This is particularly true for the problem of electromagnetic coupling between cables. Frequently, the layout and cable parameters may only be known to a certain accuracy or may vary randomly. Therefore the coupling can only be defined within statistical limits. Results have to be expressed in terms of expected values, standard deviation and confidence intervals. Calculating these limits directly is not possible as the structures are highly resonant and have a nonlinear dependence on the variables. Traditional solutions, based on the Monte Carlo approach, are not feasible as it requires millions of simulations for the multivariable problem to be solved. Unscented transforms (UT) [1] offer a way of greatly reducing the computational burden in the statistical analysis. Care also has to be taken to ensure that meaningful results are derived from the statistical analysis as the coupling involves resonances with large Q values, the maximum of which could be missed. It is far more useful to solve directly for the resonant frequencies and the depth of the resonances. In this way, the practical and significant properties of the coupling and statistical parameters can be efficiently assessed for an EMC engineer.

The theory of coaxial cable coupling is first described followed by the theory of UT in sections 2 and 3, respectively. Section 4 compares experimental results with theoretical modeling, and section 5 provides some statistical analysis.

D. W. P. Thomas (✉) · C. Christopoulos
George Green Institute for Electromagnetics,
The University of Nottingham,
Nottingham NG7 2RD, UK
e-mail: dave.thomas@nottingham.ac.uk

C. Christopoulos
e-mail: christos.christopoulos@nottingham.ac.uk

L. R. A. X. de Menezes
Departamento de Engenharia Electrica, Universidade de Brasilia,
Brasilia, Federal District 70900-970, Brazil
e-mail: Leonardo@ene.unb.br

H. J. G. Bergsma
Thales Netherlands,
Hengelo, Netherlands
e-mail: hans.bergsma@nl.thalesgroup.com

F. Leferink
University of Twente,
Enschede, Netherlands
e-mail: Frank.Leferink@UTwente.nl

2 Theory of cable coupling via the braid transfer impedance

In this work, standard single screened cables (RG58) are considered so that cable coupling will be mainly due to the transfer impedance as the transfer admittance can be neglected [2, 3]. Coupling between cables will occur when they are laid in a common path due to the voltages induced on the surface of the cable braid as the braid will not be a perfect shield. A typical cabling arrangement is as shown in Fig. 1 where the cables of length l are parallel over the majority of their length but will diverge at the terminations where they are fixed to their individual connectors. The presence of a ground plane, as depicted in Fig. 1, will also significantly affect the cable coupling. The coupling mechanism is through currents in the cable braid inducing a voltage on the other surface of the braid. The mechanism can be quantified by the transfer impedance where the induced voltage gradient E_i is given by [4]:

$$E_i(x) = Z_t I_s(x) \tag{1}$$

where I_s is the inducing current on the braid, and x is the distance along the cable.

The cable coupling equivalent circuit for the situation depicted in Fig. 1 is then as shown in Fig. 2. The source cable currents within the cable will induce a voltage gradient on the outer surface of the braid as provided in Eq. 1. The outer surfaces of the braid of the cables and the ground plane form a multiconductor transmission system called the tertiary circuit. The voltage gradient on the outer surface of the source cable will then induce currents in the tertiary circuit including a current on the outer surface of the victim cable. The current on the outer surface of the victim cable braid will in turn induce a voltage gradient within the victim cable via its braid transfer impedance which will create an induced current within the victim cable circuit. Because the coupling mechanism is relatively weak, each circuit (source, tertiary, and victim) can be solved separately. A solution for the induced current due to a distributed voltage gradient along a transmission line is given by Vance [4], and in this work this is used with the tertiary circuit being solved as a multiconductor transmission line as discussed in the Appendix. The cable coupling

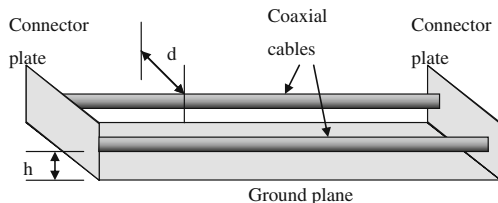


Fig. 1 Cable layout considered with two parallel cables above a ground plane

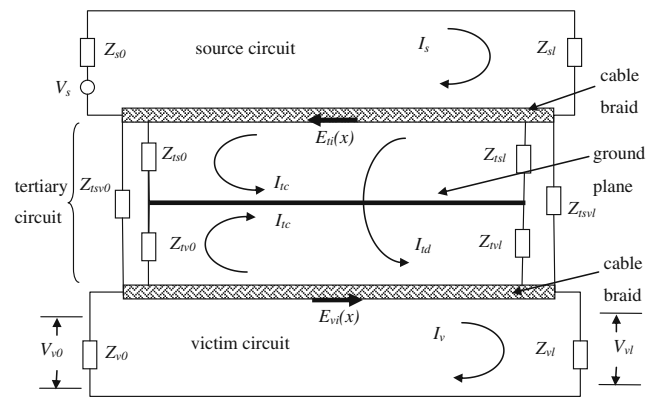


Fig. 2 Equivalent circuit for cable coupling parallel coaxial cables above a ground plane. The ground plane acts as a third conductor in the tertiary circuit

X is quantified as the ratio of received voltage on the victim cable terminal V_v (either the near end or far end) to the source cable supply voltage V_s which in dB is given as:

$$X_{dB} = 20 \log_{10} \left(\frac{V_v}{V_s} \right) \tag{2}$$

In general, the geometry of the cable layout will be variable and may even vary within manufacturing batches. The important parameters are the cable separation d , height from the ground or ground plane h , the stray reactance associated with the nature of the cable termination Z_{ts} and Z_{tv} and the cable braid transfer impedance Z_t , all of which may have a large variability. The cable braid transfer impedance is itself dependent on the manufacturing tolerances of the braid. A typical cable braid as depicted in Fig. 3 has three parameters that depend on manufacturing tolerances [5]; the lay length l , the wire diameter d , and the braid diameter D_m . It is assumed that the number of carriers N and the number of wires in each carrier are fixed for a given cable type. This gives a total of six stochastic parameters for two cables above a ground which is a relatively large number for electromagnetic problems and

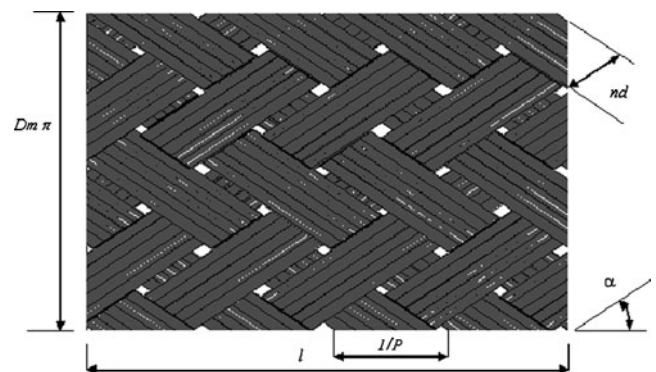


Fig. 3 Typical braid weave parameters for coaxial cables

hence a method is needed for reducing the number of calculations.

3 Theory of UT

The theory of UT was developed by Julier and Uhlman [6] where a selected set of points (sigma points) are used to approximate a nonlinear mapping. The statistics or moments (expected value, variance, kurtosis, etc.) are calculated from the weighted values at the sigma points. This method is similar to the moment design technique [7]. UT can be interpreted as an approximation of the continuous probability distribution $p()$ by a discrete distribution w_i . This produces the same moments after the nonlinear mapping:

$$E(G(\hat{u})^n) = \int (G(\hat{u})^n)p(\hat{u})d\hat{u} = \sum_i w_i G(S_i)^n \tag{3}$$

where \hat{u} is the random variable. This is analogous to the Gaussian quadrature integration scheme [1]. The sigma points and weights can be calculated from the quadrature formulae. However, for multiple random variables the Gaussian quadrature approach may require a large number of sigma points as for independent variables the resulting multidimensional polynomials are the multiplication of one-dimensional ones [1]. The number of sigma points and weights then increase to the power of the number of random variables n_{rv} . For example, if three sigma points per random variable are used then, for four random variables ($n_{rv}=4$), a total of 81 sigma points are required. In [1] an alternative method for calculating the sigma points and weights was proposed which provides a reduced set. The set of sigma points and weights satisfies the equations:

$$w_0 = 1 - \sum_i w_i$$

$$\sum_i w_i ({}_1S_i^{n_1}) \cdots ({}_{n_{rv}}S_i^{n_{n_{rv}}}) = E\{\hat{u}_1^{n_1} \cdots \hat{u}_{n_{rv}}^{n_{n_{rv}}}\} \tag{4}$$

In general, a combinatorial formulation defines the number of sigma points required [1]. Since each sigma point adds $n_{rv}+1$ unknowns to the problem, the number of sigma points N_s is the next integer of the ratio of the number of equations N_{eq} to the number of unknowns. In the case of an N th order approximation, the number of sigma points required is [1]:

$$N_s \frac{N_{eq}}{n_{rv} + 1} = \frac{1}{n_{rv} + 1} \sum_{k=1}^{2N} \frac{(n_{rv} - k + 1)!}{k!(n_{rv} - 1)} \tag{5}$$

The number of sigma points provided in Eq. 5 represents the minimum possible but this often requires a complex

solution of a large number of nonlinear equations. A simpler general set can be derived based on a geometric analogy between sigma points and points in an n_{rv} -dimensional Euclidian space [8, 9]. The set satisfies all the equations in (4) and consists of $2n_{rv}$ points located along the main axis and $2^{n_{rv}}$ points on the edges of an n_{rv} -dimensional geometric solid. The number of sigma points given by this scheme is:

$$N_s = 2^{n_{rv}} + 2n_{rv} + 1 \tag{6}$$

The weights for the $2^{n_{rv}}$ points on the edges are:

$$w_1 = \frac{n_{rv}^2}{2^{n_{rv}}(n_{rv} + 2)^2} \tag{7}$$

The weights for the $2n_{rv}$ points located along the main axis are:

$$w_2 = \frac{1}{(n_{rv} + 2)^2} \tag{8}$$

It is possible to assess if a problem with several random variables can be characterized by a smaller set of random variables by using marginal statistical probability function [9] which determines the importance of each of the variables. These distributions are essentially one-variable distributions where the calculation is performed for each variable separately. The resulting expected value and variance gives information on the significance of each of the variables. Since the UT is based on the Taylor approximation, the relative influence I_x of a variable \bar{U}_m in the variance of the result can be obtained from:

$$I_x = \frac{E\{G(\bar{U}_m)^2\} - E\{G(\bar{U}_m)\}^2}{E\{G(\bar{U}_1, \dots, \bar{U}_n)^2\} - E\{G(\bar{U}_1, \dots, \bar{U}_n)\}^2} \tag{9}$$

The UT not only provides the moments of the resulting distribution but it can also be used to derive the probability density function and cumulative density function as well. Since the UT is based on a polynomial approximation then an inverse function of the mapping can be found from a root finding procedure. For a multivariate case, the algorithm for determining the output PDF is summarized as follows:

1. Calculate the mapped denormalized sigma points.
2. Using the Moore–Penrose pseudo-inverse, calculate the coefficients of the second-order polynomial.
3. Generate the total probability density for all random variables using the polynomial calculated in (2).
4. Integrate the total probability density with respect to all variables resulting in a univariate cumulative density function (CDF) of the solution.
5. Differentiate the CDF to obtain the PDF of the solution.

4 Results

The example system chosen is where two cables of type RG58 and of length 2 m are laid along a common path above a ground plane. The cables are terminated by matched impedances and the connectors solidly earthed to common connector plates at each end. Figures 1 and 2 depict the experimental setup and the equivalent circuit. Notice that because the connectors are separated by 20 cm, there is a short section at each end where the cable separation is not constant. The source signals were in the range 100 kHz to 1 GHz and of amplitude 4 V created by a signal generator and a 36 dB amplifier. The received signals on the victim termination were measured by a spectrum analyser. Typical results for cable separation of 2 cm and a

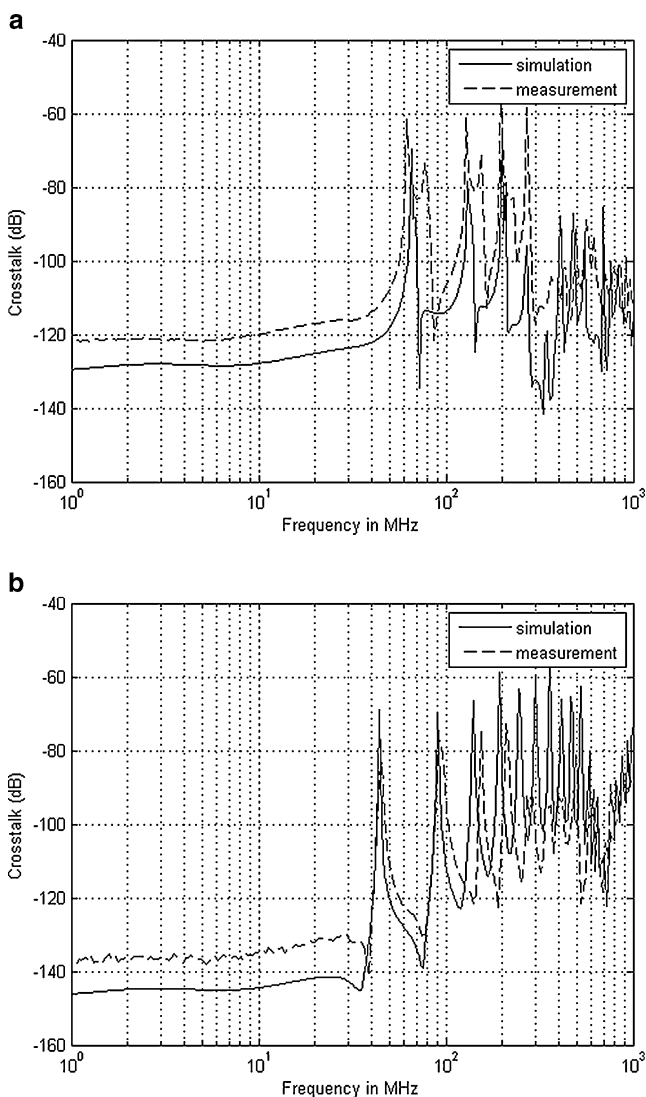


Fig. 4 Measured and theoretical crosstalk between two parallel RG58 coaxial cables of length 2 m with a 2 cm separation **a** 10 cm from the ground plane **b** cables touching the ground plane

range of cable heights are shown in Fig. 4 compared with the predicted crosstalk from solving the equivalent circuit as discussed in section 2. Agreement within 10 dB is found if the stray reactance in the tertiary terminations Z_{sv} was due to an inductance of about 0.13 μH (equivalent to the equivalent loop inductance [10]) and the stray reactance to ground (Z_s and Z_l) were negligible.

From Fig. 4, it can be seen that for low frequencies, the crosstalk can be less than -100 dB and is not of concern for engineers. For higher frequencies where resonances occur, the coupling can be significant. An important measure for cable coupling is therefore the frequency of the resonances and the peak of the cable coupling at the resonances. The peak of the coupling at resonance will be limited by the losses in the coupling circuit and the main loss will be the resistance of the outer sheath of the cables. From ref. [5] the internal impedance for an external circuit of the braid can be approximated by

$$Z_e \approx R_c \frac{(1+j)d}{\delta} \coth \frac{(1+j)d}{\delta} \quad (10)$$

where for the cable sheath: R_c is the DC resistance of the braid, d is the wire strand diameter of the braid, and δ is the conductor skin depth. This resistance is then used to define the propagation characteristics of the tertiary circuit. The resonances will have quite a high Q value.

Figure 5 shows the detail of the first resonance. It can be seen that the measurement frequencies did not include the exact resonance point, and this could also occur for the simulations. It is therefore important to establish the exact resonance frequencies in order to obtain the maximum coupling. A simpler estimation of the cable coupling can then be found by just solving directly for

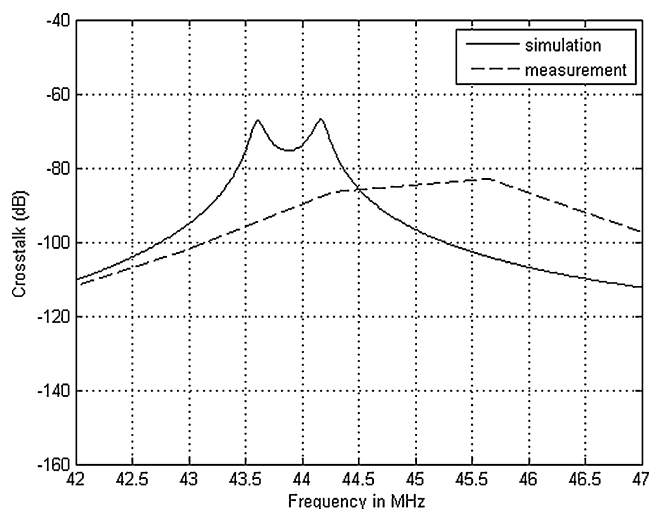


Fig. 5 Detail of the first resonance for crosstalk between two 2 m long parallel cables of 2 cm separation and touching the ground plane

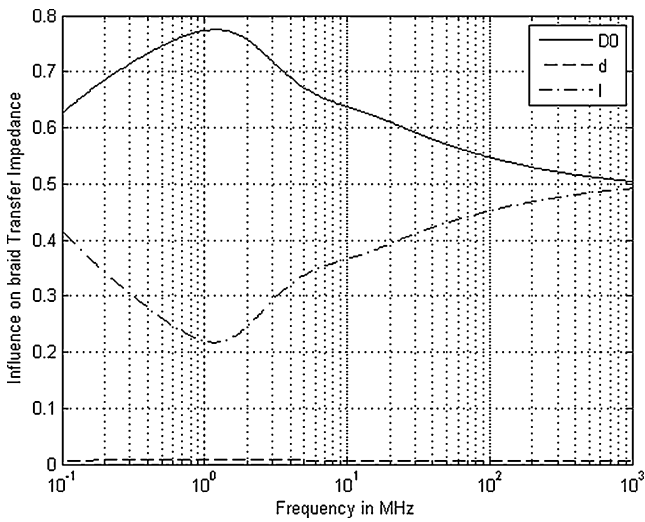


Fig. 6 Influence of the braid manufacturing tolerances on cable braid transfer impedance D0 is the cable diameter, d is the braid wire diameter and l is the laylength

the resonant frequencies and their amplitude. For the tertiary circuit, there will be a set of resonances for each mode of propagation (e.g., common mode and differential mode), and this is the reason for the two peaks seen in Fig. 5. From the theory given in the Appendix, the resonant frequencies $f_{m,n}$ (i.e., when K_1 or $K_2 \rightarrow 0$) for each mode m of propagation in the tertiary circuit will have the form:

$$f_{m,n} = \frac{c}{2\pi l} [n2\pi - \theta] \quad (11)$$

$$\theta = \arg(\rho_{0m}\rho_{lm})$$

where ρ_{0m} and ρ_{lm} are the modal termination reflection coefficients for tertiary circuit and $n=1, 2, \dots$, etc. The solution in Eq. 11 is a nonlinear problem but can be solved using a simple Newton–Raphson iteration.

In this example, the stray reactance of the tertiary circuit terminations are not precisely known and also the exact properties of the braid are only known to within the machine tolerances as discussed in the Appendix. In general, the cable height from the ground and separation may also be only known to within the cable loom

Table 1 Comparison of the standard deviation for the first resonance frequencies between Monte Carlo and the UT method

Monte Carlo		UT	
Common mode	Differential mode	Common Mode	Differential mode
1.89 MHz	1.8 MHz	1.87 MHz	1.73 MHz

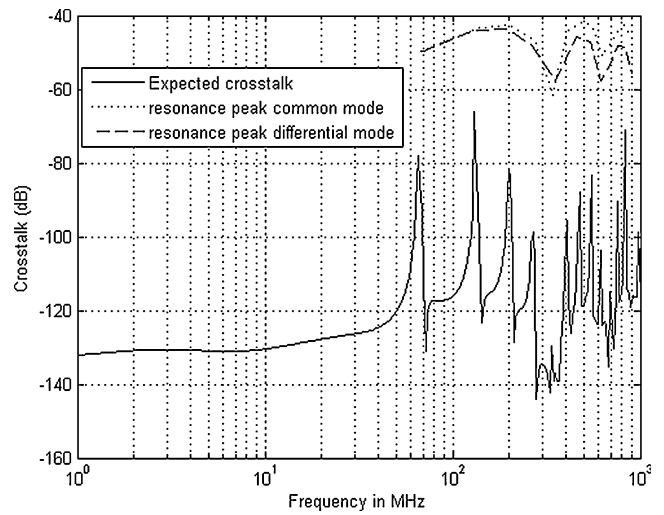


Fig. 7 Expected crosstalk and the predicted expected peak amplitudes and frequencies

construction tolerances. It will be important for EMC compliance to fully evaluate the consequences of the variability in these parameters. Not all the parameters have a significant effect, however. Using the expected manufacturing tolerances for the cable braid [5], the influence of the braid parameters on the braid transfer impedance is shown in Fig. 6. It can be seen from Fig. 6 that the influence of the variability in the braid wire diameter can be neglected. It is proposed to use the UT method to further reduce the computational burden of studying the effects of the other parameters.

The example studied is for a cable separation of 2 cm with a standard deviation of 2/3 cm, a cable height of 3 cm with a standard deviation of 1 cm, and a standard

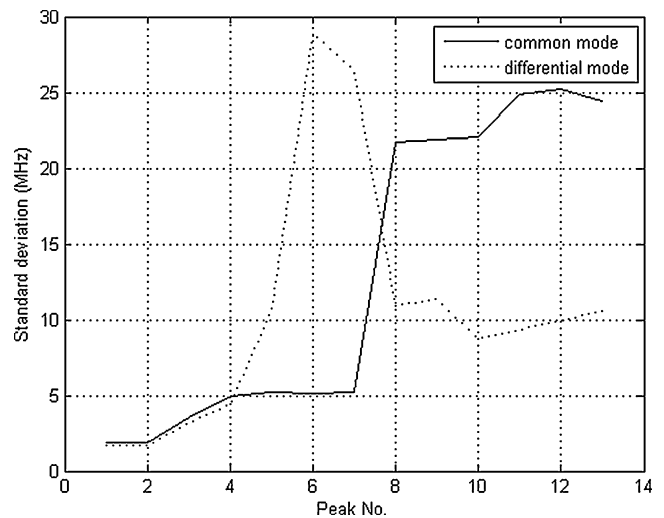


Fig. 8 The standard deviation of the resonant frequency for the two modes of propagation

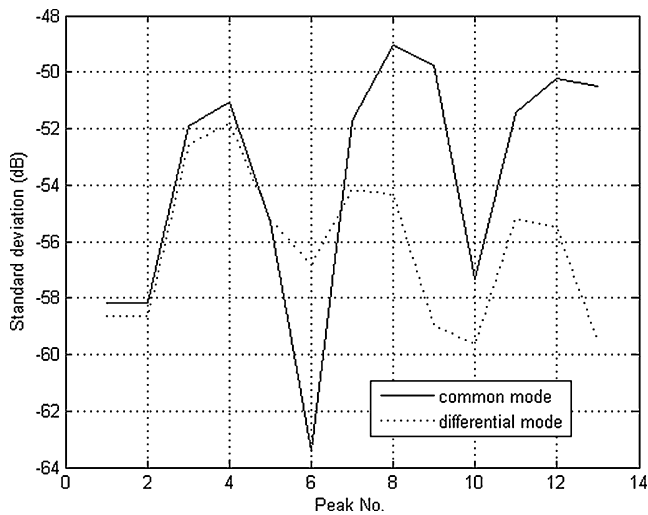


Fig. 9 Standard deviation of the resonant frequency amplitudes

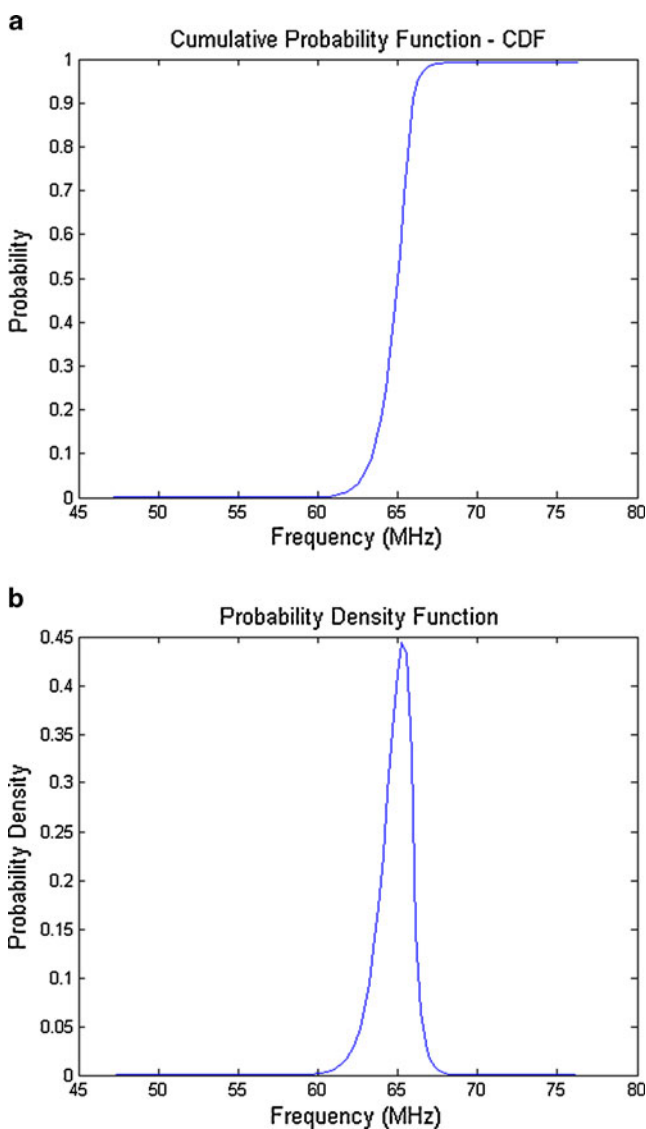


Fig. 10 Cumulative probability function (a) and probability density function (b) for the maximum crosstalk for the frequency of the first resonance (differential mode)

deviation in the estimate of the termination inductance of $0.02 \mu\text{H}$ and assuming that all the variables have a normal distribution. Table 1 shows a comparison between the UT estimation expected value and its variance of the first coupling resonance and the amplitude at that resonance compared with the Monte Carlo approach. The Monte Carlo approach used 100,000 random simulations to provide a solution (possibly needed more to converge) whereas the UT approach only required 43 sigma points (simulations) for this number of random variables (Eq. 5).

Figure 7 shows the expected value of the cable coupling as deduced using the UT over a uniform distribution of frequencies. Also shown in Fig. 7 are

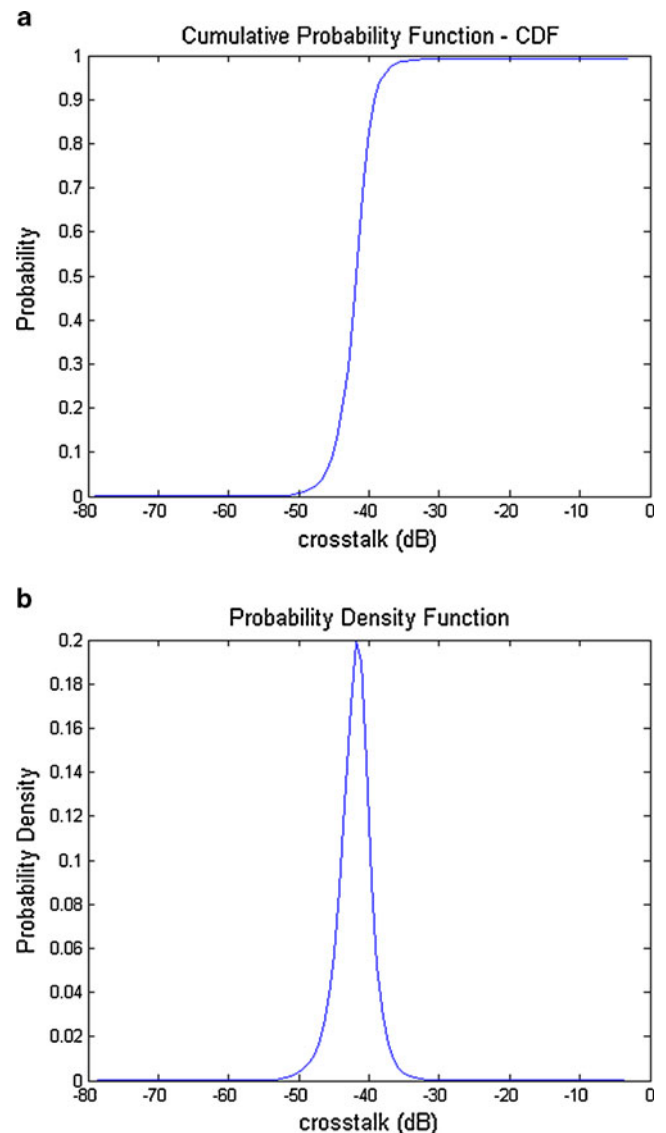


Fig. 11 Cumulative probability function (a) and probability density function (b) for the maximum crosstalk for all the resonances

Table 2 Influence of variables on the cable crosstalk (high number means strong influence)

Frequency of 1st resonance		Amplitude of first resonance		Variable
Common mode	Differential mode	Common mode	Differential mode	
0.29	0.77	0.001	0.003	$L_{\text{termination}}$
0.13	0.1	0.0007	0.0004	Height
0.58	0.12	0.0015	0.0007	Separation
0.0000001	0.000008	0.5	0.51	Lay length
0.0000016	0.005	0.49	0.49	Braid diameter

curves linking the expected resonant frequencies (found from solving Eq. 11) and their amplitude as deduced using the UT (this gives an envelope of the maximum expected coupling). Figures 8 and 9 show the standard deviation of the amplitude and frequencies of the resonances as deduced by the UT sigma points. Figures 10 and 11 show the probability distribution and cumulative probability distributions for the first two resonances. Table 2 shows the influence of the variables on the amplitude and frequency of the first resonances for the two propagation modes. From Table 2, it can be seen that the cable layout (height and separation) most strongly affects the frequency of the first resonance whereas the amplitude of the maximum crosstalk is most strongly affected by the braid parameters. This is because the resonances are limited only by the losses in the braid.

5 Conclusions

The statistical properties of cable coupling have been examined from the view point of effects due to cable manufacturing tolerances and the variability in the cable layout. It is shown that the important features to be identified are the crosstalk resonances and their amplitudes. Then, it is also shown that the UT approach can be used to provide, from a small number of simulations, a range of statistical parameters that can greatly aid in the assessment of the probable degree of cable coupling and the relative influences of the variables.

The UT method assumes that the nonlinear mapping can be accurately represented by a truncated Taylor's series, therefore, the accuracy of the UT method depends on the degree of the nonlinear mapping. For example, for time domain studies the propagation characteristics can be very nonlinear and becomes unsuitable for UT analysis [1]. In this example by studying the statistics of the resonant frequencies and their amplitudes not only does this simplify the problem but it greatly reduces the nonlinearity of the mapping studied. If the number of variables is too large, the

problem may also become unmanageable. This can be avoided by using the marginal statistical moments to identify the important variables.

Acknowledgment The authors would like to thank the EU for supporting this project through the Marie Curie program (PEM, MTKI-CT-2006-042707).

Appendix

Induced currents on multiple cable bundles

In this work the solution given by Vance [5] for the induced currents in the victim circuit or tertiary circuit is used. This just uses a one-way interaction where the effects of the victim currents on the source are neglected due to the low level of the coupling involved. For multiple coaxial cables or coaxial cables in the presence of a ground plane, the currents induced on each of the cable outer braid surfaces in the tertiary circuit will be different. The equivalent circuit is a multiconductor problem. For N cables, the governing equations will be composed of N simultaneous equations if there is a ground plane or $N-1$ simultaneous equations if a ground plane is not present. The governing equations are then:

$$\begin{aligned} \left[\frac{\partial^2 V_i}{\partial x^2} \right] - [Z][Y][V_i] &= \left[\frac{\partial E_i(x)}{\partial x} \right] \\ \left[\frac{\partial^2 I_i}{\partial x^2} \right] - [Y][Z][I_i] &= [Y][E_i(x)] \end{aligned}$$

where $[V_i]$ and $[I_i]$ are the induced voltages and currents on the tertiary circuit conductors (outer surfaces of the cable braids), $[Z]$ and $[Y]$ are the impedance matrix and the admittance matrix for the tertiary circuit conductors (here calculated as for multiconductor lines including the insulation sheath on the cables), and E_i is the induced voltage gradient along the source cable as presented in Eq. 1. These simultaneous equations can be transformed into N indepen-

dent equations of the modal voltages and currents in the tertiary circuit using $[I_{mi}] = [S]^{-1}[I_i]$ where $[S]$ is the modal transformation matrix given by the eigen vectors of $[Y][Z]$ and this gives

$$\left[\frac{\partial^2 I_{mi}}{\partial x^2} \right] - [\gamma_m]^2 [I_{mi}] = -[S]^{-1}[Y][S][E_{mi}(x)]$$

where $[\gamma_m]^2$ are the eigen values of $[Y][Z]$ and the general solution is of the form:

$$[I_{mi}(x)] = [[K_1] + [P(x)]] [e^{-\gamma_m x}] + [[K_2] + [Q(x)]] [e^{\gamma_m x}]$$

and

$$\begin{aligned} [K_1] &= [\rho_1] ([e^{\gamma_m l}] - [\rho_1][\rho_2][e^{-\gamma_m l}])^{-1} ([\rho_2][P(l)][e^{-\gamma_m l}] - [Q(0)][e^{\gamma_m l}]) \\ [K_2] &= [\rho_1][e^{-\gamma_m l}] ([e^{\gamma_m l}] - [\rho_1][\rho_2][e^{-\gamma_m l}])^{-1} ([\rho_2][Q(0)] - [P(l)]) \\ [P(x)] &= [Z_{mc}]^{-1} \left[\frac{\int_0^x e^{\gamma_m u} E_{mi}(u) du}{2} \right], [Q(x)] = [Z_{mc}]^{-1} \left[\frac{\int_x^l e^{-\gamma_m u} E_{mi}(u) du}{2} \right] \end{aligned}$$

where $[Z_{mc}]$ is the modal characteristic impedance matrix for the tertiary circuit and $[\rho_1]$ and $[\rho_2]$ are the modal reflection coefficients at the terminations of the tertiary circuit. For two identical cables, the modes reduce to the differential and common modes.

RG58 cable parameters

N	n	D0/mm	σ_{D0} /mm	d/mm	σ_d /mm	l/mm	σ_l /mm	α /rad
12	9	2.95	0.13	0.127	0.003	19.79	1.979	0.4786

References

- de Menezes L, Ajayi A, Christopoulos C, Sewell P, Borges GA (2008) Efficient computation of stochastic electromagnetic problems using unscented transforms. *IET Sci Meas Technol* 2(2):88–95
- Benson FA, Cudd PA, Tealby JM (1992) Leakage from coaxial cables. *IEE Proc-A* 139(6):285–303
- Sali S (1993) A circuit based approach for crosstalk between coaxial cables with optimum braided shields. *IEEE Trans EMC* (2): 300–311
- Vance EF (1978) Coupling to shielded cables. Wiley, New York. ISBN 0-471-04107-6
- Kley T (1993) Optimised single braided cable shields. *IEEE Trans EMC* 35(1):1–9
- Julier SJ, Uhlmann JK (2004) Unscented filtering and nonlinear estimation. *Proc IEEE* 92(3):401–422
- Zhang J (2006) The calculating formulae and experimental methods in error propagation analysis. *IEEE Trans on Reliability* 55(2):169–181
- De Menezes LRAX, Thomas DWP, Christopoulos C, Ajayi A, Sewell P (2008) The use of unscented transforms for statistical analysis in EMC. In: *Int Symposium on Electromagnetic Compatibility-EMC Europe*, 8–12 Sept 2008. pp. 1–5
- De Menezes LRAX, Thomas DWP, Christopoulos C (2009) Statistics of the shielding effectiveness of cabinets. In: *Proceedings of the ESA Workshop on Aerospace EMC*. Florence, Italy, 1 April–30 March
- Jackson JD (1998) *Classical electrodynamics*, 3rd edn. Wiley, New York. ISBN 0-471-30932-X